



Development and characterization of a green procedure for apigenin extraction from *Scutellaria barbata* D. Don

Yu-Chiao Yang^{a,b}, Ming-Chi Wei^{c,*}

^a Department and Graduate Institute of Pharmacology, Kaohsiung Medical University, Kaohsiung 80708, Taiwan

^b Department of Medical Research, Kaohsiung Medical University Hospital, Kaohsiung 80708, Taiwan

^c Department of Applied Geoinformatics, Chia Nan University of Pharmacy and Science, Tainan 71710, Taiwan



ARTICLE INFO

Keywords:

Scutellaria barbata D. Don
Apigenin
Supercritical CO₂ extraction
Ultrasound-assisted extraction
Second-order kinetic model
Eyring transition state theory
Green alternative procedure
Theoretical solubility

ABSTRACT

This study compared the use of ultrasound-assisted supercritical CO₂ (USC-CO₂) extraction to obtain apigenin-rich extracts from *Scutellaria barbata* D. Don with that of conventional supercritical CO₂ (SC-CO₂) extraction and heat-reflux extraction (HRE), conducted in parallel. This green procedure yielded 20.1% and 31.6% more apigenin than conventional SC-CO₂ extraction and HRE, respectively. Moreover, the extraction time required by the USC-CO₂ procedure, which used milder conditions, was approximately 1.9 times and 2.4 times shorter than that required by conventional SC-CO₂ extraction and HRE, respectively. Furthermore, the theoretical solubility of apigenin in the supercritical fluid system was obtained from the USC-CO₂ dynamic extraction curves and was in good agreement with the calculated values for the three empirical density-based models. The second-order kinetics model was further applied to evaluate the kinetics of USC-CO₂ extraction. The results demonstrated that the selected model allowed the evaluation of the extraction rate and extent of USC-CO₂ extraction.

1. Introduction

Scutellaria barbata D. Don is popularly used in China not only as a traditional Chinese medicine for the treatment of various diseases (Yang, Wei, Hong, Huang, & Lee, 2013; Tao & Balunas, 2016) but also as a tea for health maintenance (Zhao, Deng, Chen, & Li, 2013). Apigenin is among the major bioactive flavonoids purified from *S. barbata* D. Don that contribute to plant pharmacological efficacy. Flavonoids have minimal toxicity and have many important pharmacological activities, including antitumor, hepatoprotective, antibacterial, anti-diabetes, anti-inflammatory and antioxidant activities and the ability to reduce the risk of cardiovascular diseases (Wei, Yang, Chiu, & Hong, 2013; Xie et al., 2017; Yang, Wei, Huang, Lee, & Lin, 2013; Yang, Wei, Huang, & Lee, 2013).

Several techniques have been used to extract flavonoids from plant matrices, including maceration (Albuquerque et al., 2017), supercritical CO₂ extraction (SC-CO₂) (Martinez-Correa et al., 2017), heat-reflux extraction (HRE) (Yang, Wei, Huang, et al., 2013; Wei et al., 2013; Bosso, Guaita, & Petrozziello, 2016), ultrasound-assisted extraction (UAE) (Yang, Wei, & Huang, 2012; Albuquerque et al., 2017; Moorthy et al., 2017), microwave extraction (Albuquerque et al., 2017; Xie et al., 2017) and pressurized hot water extraction (Liau, Ponnusamy, Lee, Jong, & Chen, 2017). Among these techniques, SC-CO₂ has attracted interest for its effective

extraction of bioactive compounds from various types of matrices to provide relatively clean and high-quality extracts (Abrahamsson, Rodriguez-Meizoso, & Turner, 2015; Santos, Aguiar, Barbero, Rezende, & Martínez, 2015; Yang, Ling, & Wei, 2017). The most important advantages of SC-CO₂ are its excellent mass transfer properties, facile separation of the solvent from the extracted material, use of milder operating conditions, reduced need for environmentally aggressive solvents (thus reducing their use and disposal) and ease of control by altering the temperature, pressure or use of a cosolvent. Despite the advantages of SC-CO₂ extraction, however, it has the limitation of requiring high-pressure equipment, which is susceptible to failed mechanical stirring, potentially resulting in a substantial decrease in the extraction efficiency. In the pursuit of the required extraction yields with shorter processing times or with greater economic efficiency, ultrasound-assisted supercritical CO₂ (USC-CO₂) extraction is of growing importance because it can achieve good extraction efficiency and appropriate selectivity under less severe operating conditions. Recently, there have been several attempts to apply this green procedure to extract compounds of interest from various raw materials (Hu, Zhao, Liang, Qiu, & Chen, 2007; Glisic, Ristic, & Skala, 2011; Wei, Xiao, & Yang, 2016; Wei, Lin, Hong, Chen, & Yang, 2016). The enhancements in the extraction efficiency might be due to the cavitation and thermal effects induced by ultrasonic waves (Wei & Yang, 2015; Wei, Lin, et al., 2016; Moorthy et al., 2017).

Solubility data for solutes in SC-CO₂ are essential for the

* Corresponding author.

E-mail address: s120702@mail.cnu.edu.tw (M.-C. Wei).

development of models for the extraction processes. Knowledge about solute solubility in SC-CO₂ permits the selection of ranges for the conditions to provide essential information for the engineering process required to extract the final pharmaceutical product. Therefore, solubility measurements are necessary and have received considerable attention. Furthermore, correlations and predictive techniques are also essential to generate experimental data.

The main purpose of this work was to develop effective conditions for the separation of apigenin from *S. barbata* D. Don using a combinatory procedure. The effects of ultrasonic energy, temperature, pressure, cosolvent percentage, time, and CO₂ flow rate on yield were estimated using single-factor experiments to compare the contents of apigenin in different extracts and to determine the optimal conditions for the extraction of apigenin from *S. barbata* D. Don. A reverse-phase high-pressure liquid chromatography (HPLC) system coupled with a UV detector and HPLC combined with tandem mass spectrometer detection (HPLC-MS) were used to quantify the level of apigenin in the extracts. Finally, the experimental solubility data were fitted with three semi-empirical models. HRE, SC-CO₂ and USC-CO₂, optimized for the quality and quantity of apigenin produced, were also compared and analyzed comprehensively. In addition, the second-order kinetic model and the Eyring transition state theory were applied to examine the kinetics of USC-CO₂ extraction (Swati, Haldar, Ganguly, & Chatterjee, 2013).

2. Materials and methods

2.1. Plant materials

S. barbata D. Don (SD3) samples were purchased from local Chinese medicinal shops (Kaohsiung, Taiwan) and were identified by Kaiser Pharmaceutical Limited Company (KPC, Tainan, Taiwan). The samples were pulverized (0.36 mm) and analyzed to determine the moisture contents (13.08%) by drying at 105 °C to a constant mass (Yang, Wei, Hong, et al., 2013; Yang & Wei, 2016). These values were used to express the extraction yield as the ratio of the mass of the extracted material (mg) to the mass of the dried plant loaded in the extraction vessel (g).

2.2. Solvents and reagents

Apigenin was purchased as an HPLC reference standard from Acros Organics (Morris Plains, NJ, USA). Methanol, ethanol, acetone, acetonitrile, ethyl acetate, *n*-hexane and phosphoric acid were bought from Merck Co. (Darmstadt, Germany). Deionized water was prepared using a Milli-Q reverse osmosis unit from Millipore (Bedford, MA, USA).

2.3. HPLC and HPLC-MS analysis

HPLC analysis of the target compounds was conducted on a Jasco HPLC system (Jasco, Tokyo, Japan) with a LiChrospher® C₁₈ analytical column (Merck, Darmstadt, Germany) and a Jasco MD-910 intelligent ultraviolet/visible (UV/vis) multi-wavelength detector. The injection volume for all samples was 20 µL. The quantitative evaluation of apigenin was further performed with a calibration curve (linear range, 60–320 µg/mL). More details about the equipment and its separation conditions can be found in a previous work (Wei et al., 2013).

A Waters liquid chromatography system (Waters 2695 Separations Module, Waters Corporation, MA, USA) connected to an MS detector (HPLC-MS system) was used to identify the compounds. Chromatographic separations were performed on a ZORBAX Eclipse XDB-C18 column, Narrow Bore RR 2.1 × 150 mm, 3.5 µm particle size. Mass spectra were acquired using a quadrupole mass analyzer (Waters Micromass ZQ), equipped with an electrospray ionization (ESI) probe and working in the negative mode. Cone voltage fragmentation was at 20 V, the capillary voltage was 3 kV, the desolvation temperature was 200 °C, the source temperature was 120 °C, and the extractor voltage

was 12 V. The flow rate was 0.2 mL/min, the injection volume was 40 µL, and the column temperature was maintained at 25 °C. The mobile phase consisted of 0.02% formic acid in H₂O (solvent A, water-formic acid, 100: 0.02, v/v) and 0.02% formic acid in methanol (solvent B, methanol-formic acid, 100: 0.02, v/v), and the following gradient was used: 0–2.5 min, 95% (solvent A); 2.5–50 min, 95–0% (solvent A); 50–70 min, 0% (solvent A). The mass spectra and retention indices of the target compounds in the extracts were compared with those of the pure compounds.

2.4. Ultrasound-assisted supercritical CO₂ (USC-CO₂) extraction

For each experiment, 20 g of dried-powdered *S. barbata* D. Don (SD3) mixed with 2-mm stainless steel balls was placed in a steel cylinder plugged with glass wool on both ends. The loaded cylinder, connected to a heating coil, was then introduced into the SC-CO₂ extraction apparatus (Yang & Wei, 2016). UAE (75% duty cycle) was combined and performed by placing the loaded cylinder in an ultrasonic bath (fixed at the same position in the bath) with a working frequency of 40 kHz and power of 185 W (Branson B-33810E-DTH, USA). Samples were extracted in the static mode for 15 min (ultrasound assisted), followed by dynamic extraction for 5 to 280 min (ultrasound assisted) at a CO₂ flow rate of 0.17–0.83 g/min with 11.6% (v/v) aqueous ethanol (80%, v/v) as cosolvent. Further details on the equipment and its operation are the same as those described by Yang and Wei (2015a, 2016).

2.5. Conventional solvent extraction

The heat-reflux extraction (HRE) process was conducted at 75 °C for 60 min using acetone, ethanol, *n*-hexane and water as the solvent. More details about its extraction conditions can be found in a previous work (Yang, Wei, Huang, et al., 2013; Wei & Yang, 2014).

2.6. Statistical analysis

All yields were calculated, and composition analyses were performed on a moisture-free basis. The mean and the standard deviation (SD) of the mean were calculated from 6 experiments. The results are expressed as the mean ± SD. Analysis of variance (ANOVA) was performed using Tukey's method with a significance level of $p < 0.05$ using Microsoft Excel 2010 (Microsoft, USA) and Origin software version 6.1 (Origin Lab Software, Northampton, MA, USA). Furthermore, the concordance between the experimental data and the calculated value was established by the average absolute relative deviation (AARD) and the coefficient of determination (R^2), which were calculated using the following equations:

$$AARD(\%) = \frac{100}{n} \sum_{i=1}^n \left| \frac{y_{p,i} - y_{e,i}}{y_{e,i}} \right| \quad (1)$$

$$R^2 = 1 - \frac{\sum_{i=1}^n (y_{e,i} - y_{p,i})^2}{\sum_{i=1}^n (y_{e,i} - y_m)^2} \quad (2)$$

where $y_{p,i}$ and $y_{e,i}$ are the predicted and experimental solubility values, respectively. y_m is the mean solubility value, and n is the number of experimental runs.

3. Results and discussion

3.1. Total extract

To measure the solubility of a solute in CO₂ using the dynamic method, determining an adequate CO₂ flow rate in USC-CO₂ extraction

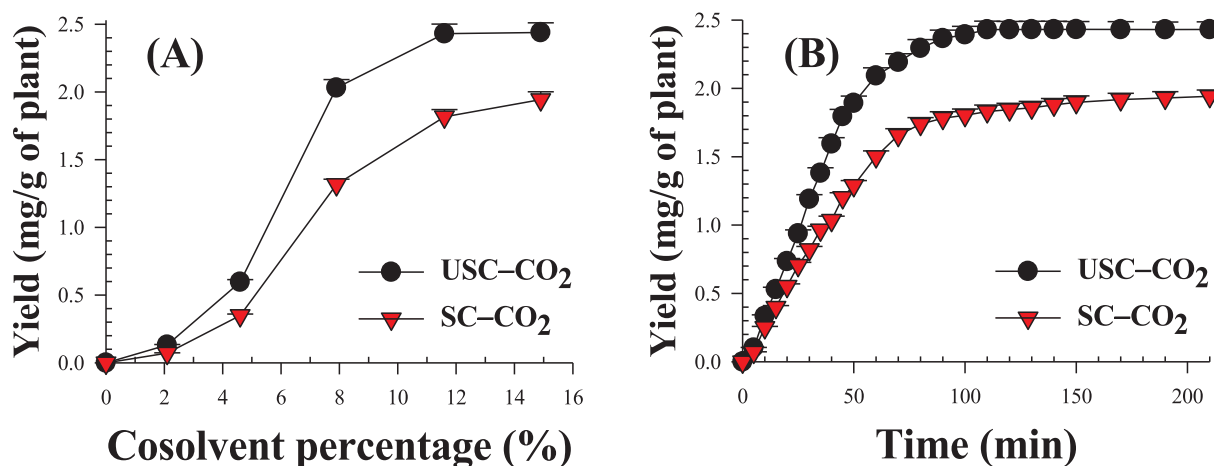


Fig. 1. Effects of (A) cosolvent percentage and (B) dynamic extraction time on the extraction yield of apigenin by using USC-CO₂ and SC-CO₂ extraction.

is a crucial factor because it can affect the extraction yield and the selectivity of the supercritical fluid. To use the dynamic method to assess experimental solubility values, the solvent flow rate must be sufficiently low to guarantee adequate contact time between the phases, ensuring solvent saturation. The overall extraction curves (OECs) of the USC-CO₂ extraction of *S. barbata* D. Don at different CO₂ flow rates are presented in S. 1A. The experimental results highlighted that the CO₂ flow rate affected the OECs. As shown in S. 1A, the yield of total extract increased with increasing CO₂ flow rate from 0.17 g/min to 0.83 g/min. After 110 min (5.197 g CO₂/g dry plant) of USC-CO₂ extraction at 32 °C and 35 MPa, the total extract obtained at 0.83 g/min (7.5%, g extracted/g dry plant) was almost 2.9 times higher than that obtained at 0.17 g/min (2.6%, g extracted/g dry plant).

The OECs of *S. barbata* D. Don from the USC-CO₂ experimental data (S. 1A) were fitted to a spline using two straight lines. The first line was associated with the constant extraction rate (CER) period. The slope of the CER period was calculated, and the results were expressed by Y_{CER} , the solute concentration in the solvent phase (g extracted/g CO₂). The effect of the CO₂ flow rate on determining the solubility of *S. barbata* D. Don in SC-CO₂ is presented in S. 1B for assays performed at 35 MPa and 32 °C. The results show the slope of the straight line adjusted to the CER period, also called Y_{CER} , for extractions performed at various CO₂ flow rates. S. 1B shows that the value of Y_{CER} increases with increasing CO₂ flow rate (0.49 g/min) up to a maximum and then decreases. At saturation, the Y_{CER} in the fluid phase at the bed outlet should be at a maximum. Therefore, the CO₂ flow rate of 0.49 g/min, which corresponds to this maximum, is suitable for measuring solubility.

A temperature and pressure of 32 °C and 35 MPa were chosen to determine the flow rate values at which saturation values become independent of the flow rate because within this study, under such conditions, SC-CO₂ reaches its highest density (961.72 kg/m³). Thus, when such flow rates are applied in other experiments to investigate the solubility of compounds in SC-CO₂, the saturation of the solute in SC-CO₂ is ensured, regardless of the other conditions being applied. Therefore, all subsequent extraction and solubility measurements in this study were performed at a SC-CO₂ flow rate of 0.49 g/min.

3.2. Chromatogram

The apigenin content in extracts obtained from HRE, SC-CO₂ extraction and USC-CO₂ extraction was identified and quantified with HPLC and LC-MS. A typical HPLC chromatogram of the apigenin standard solution was compared with the chromatograms from extracts obtained from the optimized HRE and USC-CO₂ extractions in S. 2. The chromatograms at 280 nm for both extracts, one obtained by USC-CO₂ extraction at 56 °C and 30 MPa and the other obtained by conventional

HRE ethanolic extraction, and the peak of the marker with no interference at the elution time of the analyte all correspond to apigenin. The identities of the peaks for apigenin in both samples were verified by comparing their retention times and UV absorption spectra with those of a standard. Furthermore, the results indicated that apigenin was the most abundant compound in the USC-CO₂ extracts of *S. barbata* D. Don (S. 2C)

3.3. Effects of USC-CO₂ extraction conditions on extraction yield

The influence of ultrasound on the quality of apigenin was evaluated by comparison with HRE based on HPLC measurement (S. 2B and C), and no effect on the quality of the natural component was found. Therefore, the USC-CO₂ method was chosen to extract apigenin from *S. barbata* D. Don in this study due to its efficacy and straightforward handling (Wei, Xiao, et al., 2016). Based on the HRE results, 80% (v/v) aqueous ethanol was used as a cosolvent due to its safety for the food, pharmaceutical and biotechnology industries and its improved solubilizing capacity for apigenin. Other parameters, such as a mean particle size of 0.36 mm and a static extraction time of 15 min (with ultrasound), were found to be appropriate for USC-CO₂ extraction (Yang & Wei, 2016) and were selected as constant parameters in the following experiments. In addition, the UAE was fixed at an ultrasonic frequency of 40 kHz, a power of 185 W and an ultrasound cycle of 75% (intermittent sonication).

3.3.1. The effect of cosolvent percentage

The effect of cosolvent percentage on the yield of apigenin is presented in Fig. 1A. The extraction yield of apigenin in USC-CO₂ extraction increased with increasing cosolvent percentage from 2.1 to 11.6 but did not conspicuously change from 11.6 to 14.9%. However, the extraction yield increased significantly with increasing cosolvent percentage from 2.1 to 14.9% in conventional SC-CO₂ extraction (Fig. 1A).

The yield of apigenin in USC-CO₂ at an extraction temperature of 56 °C with 6.3 mL of 80% ethanol for 125 min was approximately 1.3 times higher than that obtained by conventional SC-CO₂ extraction at an extraction temperature of 64 °C with 15 mL of 80% ethanol for 210 min (Fig. 1A and Table 1). These results suggest the advantages of USC-CO₂ extraction, which can achieve a higher yield at a lower pressure, temperature and solvent volume and can efficiently reduce extraction time compared with the conventional SC-CO₂ extraction method. The higher efficiency of the USC-CO₂ extraction can be explained by the mechanical action of ultrasonication, which could accelerate swelling and hydration and cause enlargement of the pores in the plant cell walls. Therefore, USC-CO₂ extraction resulted in better mass transfer of the solute constituents from the plant materials to the

Table 1
Comparison of the extraction conditions and extraction yields of apigenin obtained by the heat-reflux extraction (HRE), SC-CO₂ extraction and USC-CO₂ extraction.

Extraction parameters	Extraction mode		
	HRE	SC-CO ₂ extraction	USC-CO ₂ extraction
Herbal sample	SD3	SD3	SD3
Mean particle size (mm)	0.36	0.36	0.36
Plant weight (g)	20	20	20
Stirring rate (rpm)	300	—	—
Static extraction time (min)	—	30	15
Dynamic time (min)	—	210	110
Extraction time (min)	300	240	125
Extraction temperature (°C)	75	64	56
Extraction pressure (MPa)	—	35.0	30.0
Liquid/solid ratio (mL/g)	16	—	—
CO ₂ flow rate (g/min)	—	0.49	0.49
Extraction cycles	5	—	—
Duty cycle of ultrasound exposure (%)	—	—	75%
Percentage of cosolvent (80% ethanol) in SC-CO ₂ (% v/v)	—	14.9	11.6
Yield of apigenin (mg/g) ^a	1.662 ± 0.069	1.943 ± 0.079	2.431 ± 0.097
Ethanol (% v/v) ^b	80%	—	—

^a Values are written as the mean ± SD of six replications and are calculated based on plant dry weight basis (SD3).

^b Ethanol concentration in water (% v/v).

solvent. The influence of microjets on the plant cells after the collapse of cavitation bubbles could increase the rate of solvent penetration into the plant tissue and result in increased accessibility and extractability of the extracts. Similar outcomes have been reported previously (Santos et al., 2015; Wei, Lin, et al., 2016).

3.3.2. Efficiency of ultrasonic energy and extraction time

The effects of ultrasonic energy and dynamic extraction time on the extraction yields of apigenin from *S. barbata* D. Don are shown in Fig. 1B. The results indicate that, in both USC-CO₂ extraction and traditional SC-CO₂ extraction, the extraction yield is highly time-dependent. The amount of apigenin extracted increased with the dynamic extraction time up to 110 min for USC-CO₂ extraction and up to 210 min for traditional SC-CO₂ extraction. However, the yield of apigenin did not vary significantly with time after those time points, i.e., there was no change in the yield from 110 to 220 min for USC-CO₂ extraction and from 210 to 220 min for traditional SC-CO₂ extraction. Therefore, the appropriate dynamic extraction time was found to be 110 min for USC-CO₂ extraction and 210 min for traditional SC-CO₂ extraction. Compared with traditional SC-CO₂ extraction, UAE combined with SC-CO₂ extraction was found to enhance the yield of the desired compound in less time. With the application of ultrasound to both the static stage and dynamic stage of SC-CO₂ extraction, these enhancements might be attributable to ultrasonic cavitation, which could accelerate swelling and hydration and enlarge the pores in the plant cell walls. These processes could increase the mass transfer of solute constituents from the plant materials to the SC-CO₂ solvent to more effectively release the analyte. These results supported previous findings that the application of ultrasound during supercritical fluid extraction processes can accelerate the extraction rate and improve the yield (Klejduš, Lojtková, Plaza, Šnóbllová, & Stěrbová, 2010; Santos et al., 2015). A recent similar work also found an increase in the extraction efficiency as a result of USC-CO₂ extraction compared with the conventional method (Hu et al., 2007).

3.3.3. The effects of temperature and pressure

The importance of the effects of extraction pressure and temperature in the SC-CO₂ extraction of target compounds from raw matrices has been emphasized in the literature, as the optimization of these two variables can lead to higher extraction efficiency and selectivity for compounds of interest in the supercritical solvent (Abrahamsson et al., 2015; Marcello et al., 2015). The experimental data are illustrated in Fig. 2A–J, showing the variation in the yield of apigenin with the

amount of SC-CO₂ used under these experimental conditions. The extraction pressure was one of the critical factors influencing the extraction yield of apigenin, which increased markedly with pressure from 12.5 to 30.0 MPa. This effect of pressure is due to the increase in carbon dioxide density, which decreases the distance between the molecules and thus increases the interaction between the analytes and CO₂, enhancing the extraction efficiency of the target compounds in both USC-CO₂ extraction and conventional SC-CO₂ extraction. Similarly, most of the previous literature surveyed indicates that an increase in the extraction pressure of SC-CO₂ leads to an increase in the amount of target compounds obtained from various matrices (Taher et al., 2014; Tomita et al., 2014; Yang, Wei, & Hong, 2014). Nevertheless, a less significant effect on USC-CO₂ extraction yields can be observed in Fig. 2A and B for operating pressures ranging from 30.0 to 35.0 MPa. This effect may result from a decrease in diffusivity, which makes it difficult for molecules to diffuse into the solid's pores to dissolve the analyte, and to a reduction of the free space in the solid owing to the greater condensation of the solid matrix at higher pressure (35.0 MPa). Thus, the decreases in diffusivity and in the void fraction should play more important roles in the result at 35.0 MPa than the increase in density. Similar outcomes have been reported by many studies (Macías-Sánchez et al., 2009; Tomita et al., 2014; Gao, Nagy, Liu, Simándi, & Wang, 2009; Wei, Hong, & Yang, 2017). However, the extraction yield increased significantly with increasing pressure from 12.5 to 35.0 MPa min in conventional SC-CO₂ extraction (Fig. 2F–J). The higher efficiency of the USC-CO₂ extraction can be explained by the turbulence and acoustic streaming induced by ultrasound, which can significantly increase the solid–liquid mass transfer coefficients to increase the yield.

As shown in Fig. 2, these two different effects of temperature on the yield were observed in both the USC-CO₂ extraction and the conventional SC-CO₂ extraction of apigenin from *S. barbata* D. Don. At the lower pressure of 12.5 MPa, the extraction yield decreased with increasing temperature from 32 to 64 °C, but at higher pressures (19.5 to 35.0 MPa), an inverse trend was observed. Similar results have been reported in the earlier literature (Khamda, Hosseini, & Rezaee, 2013; Tomita et al., 2014). At a lower pressure (12.5 MPa), the SC-CO₂ density can be greatly decreased by increasing the temperature, which results in an overall tendency to decrease the efficiency of both the USC-CO₂ extraction and conventional SC-CO₂ extraction as the temperature rises. On the other hand, at higher pressures (19.5, 25.0, 30.0 and 35.0 MPa), the decreasing SC-CO₂ density as a result of increasing temperature may not overcome the increasing vapor pressure of the

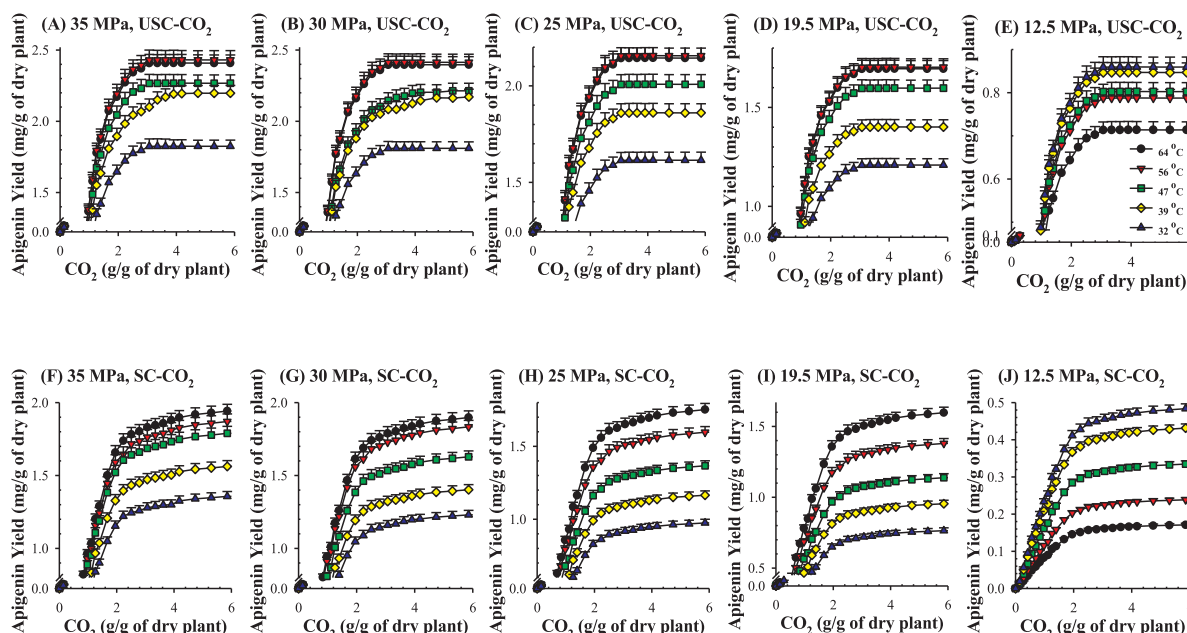


Fig. 2. The cumulative yield of apigenin for the (A–E) USC-CO₂ and (F–J) SC-CO₂ dynamic extractions at a CO₂ flow rate of 0.49 g/min, 32–64 °C and 12.5–35 MPa.

solutes and the molecular interactions of the supercritical phase; therefore, there is an overall tendency toward improved extraction efficiency as the temperature rises. However, a temperature increase from 56 to 64 °C at these four higher pressures caused a slight decrease in the extraction yield for apigenin (Fig. 2A–D). This decrease is ascribed to a decrease in the SC-CO₂ density with increasing temperature, which dominates over the increase in solute vapor pressure and the desorption of solutes from the active sites by SC-CO₂ at this specific pressure. Consequently, a temperature of 56 °C was selected as the best extraction temperature for USC-CO₂ extraction in this study. There seems to be, therefore, a balance between the two apparently contradictory effects of temperature, resulting in a crossover tendency in the USC-CO₂ extraction of apigenin from *S. barbata* D. Don. Similar phenomena have generally been observed in solid-supercritical fluid systems (Tomita et al., 2014; Taher et al., 2014; Khamda et al., 2013). However, the extraction yield of apigenin increased when the temperature increased from 32 to 64 °C during traditional SC-CO₂ extraction (Fig. 2F–H). Compared to the traditional SC-CO₂ extraction method, USC-CO₂ extraction reduced the extraction temperature and pressure while also achieving superior yields of apigenin and provides a good alternative to such processes for industrial production.

Furthermore, the conventional HRE method was conducted in parallel for comparison, and the results are shown in Table 1. It shows that USC-CO₂ extraction not only had the highest extraction yield but also required less time, a lower temperature and a reduced amount of solvent than were necessary for HRE. Under the optimal experimental conditions (Table 1), the highest apigenin yield (2.431 ± 0.097 mg/g of dry plant) was obtained via USC-CO₂ extraction with 6.3 mL aqueous ethanol (80%, v/v) as the cosolvent under the following conditions: low pressure (30.0 MPa) and temperature (56 °C) with a short extraction time (125 min). This result proved that USC-CO₂ extraction can serve as an alternative to conventional organic solvent extraction methods. Therefore, USC-CO₂ extraction seems to be the best method for the extraction of the target compound from *S. barbata* D. Don from the perspective of yield and extraction efficiency. All these characteristics of the combined process make it very popular in the fields of functional food, pharmaceutical and biotechnology.

3.4. Theoretical solubility determination

The quantitative analysis of the extract (S. 2) showed that apigenin is present in larger amounts under all conditions. Accordingly, the extract solubility for the pseudoternary system is governed by the solubility of apigenin in SC-CO₂. According to previous representative studies (Wei, Xiao, et al., 2016; Wei, Lin, et al., 2016), the theoretical solubility of apigenin in SC-CO₂ can be determined from the slope of the initial linear portion of the apigenin curves in *S. barbata* D. Don extracts (Fig. 2), which are summarized in Table 2. The reported results are expressed in terms of the equilibrium solubility, Y_{apigenin}^* (g apigenin/g CO₂), of apigenin in this supercritical fluid system under pressures ranging from 12.5 to 35 MPa and operating temperatures ranging from 32 to 64 °C. Each data point represents the average of at least six runs, and the relative SD between measurements ranged from 3.1 to 5.8%. The effect of pressure on the theoretical solubilities of apigenin reflected expected trends, with elevated pressure increasing solubility at all temperatures. As the pressure is increased at a constant temperature, the density of SC-CO₂ increases, thereby increasing the interactions between the apigenin and CO₂ molecules, which results in a stronger solvation power for SC-CO₂. As shown in Table 2, theoretical solubility increases with pressure, especially at lower pressures, as demonstrated by the slightly steeper slope, whereas the effect is less pronounced at higher pressures, as shown by the slightly gentler slope. This result might be explained by the fact that the density of SC-CO₂ is more sensitive to pressure, especially at lower pressures, as shown in Table 2.

Another main factor affecting the theoretical solubility of apigenin is the system temperature, which affects the solubility in two opposite ways. At a lower pressure of 12.5 MPa, the theoretical solubility decreases slightly with increasing temperature; conversely, at higher pressures (19.5, 25.0, 30.0 and 35.0 MPa), the theoretical solubility begins to increase with increasing temperature. As previously shown, these results are most likely due to the opposing effects of solvent density and solute vapor pressure on the solubility. The effects of temperature on the two parameters are complicated; as a result, the theoretical solubility of apigenin in the supercritical fluid system exhibits a crossover phenomenon. It is clearly from Table 2 that the

Table 2

Solubility measured by the dynamic USC-CO₂ extraction at various temperatures and pressures for the pseudo-ternary system.

T (°C)	P (MPa)	ρ^a (kg/m ³)	$Y^*_{\text{apigenin}} \times 10^4$ (g apigenin/g CO ₂)
32	12.5	793.575	5.366 ± 0.209
	19.5	876.863	7.547 ± 0.302
	25.0	914.620	10.083 ± 0.504
	30.0	941.040	11.302 ± 0.552
	35.0	961.715	11.392 ± 0.568
39	12.5	716.999	5.287 ± 0.217
	19.5	845.730	8.748 ± 0.326
	25.0	880.074	11.614 ± 0.517
	30.0	910.430	13.015 ± 0.564
	35.0	935.112	13.121 ± 0.570
47	12.5	587.555	5.011 ± 0.206
	19.5	801.306	9.974 ± 0.383
	25.0	848.720	12.537 ± 0.528
	30.0	883.000	13.343 ± 0.578
	35.0	908.340	14.157 ± 0.583
56	12.5	482.417	4.917 ± 0.202
	19.5	749.332	10.635 ± 0.409
	25.0	806.540	13.461 ± 0.554
	30.0	846.726	15.073 ± 0.605
	35.0	875.151	15.179 ± 0.534
64	12.5	418.487	4.456 ± 0.165
	19.5	724.872	10.585 ± 0.403
	25.0	767.592	13.386 ± 0.536
	30.0	809.550	14.964 ± 0.598
	35.0	843.416	15.038 ± 0.558

^a Density of the SC-CO₂.

^b Y^*_{apigenin} : the theoretical solubility of apigenin in SC-CO₂.

theoretical solubility increases with increasing temperature over the pressure range of 19.5 to 35.0 MPa, meaning that in the current experimental pressure range, the influence of temperature on solute vapor pressure exerted more dominant effects on solubility than do changes in the density of the system. However, at the lower pressure of 12.5 MPa, the ability of a higher temperature to decrease the density of SC-CO₂ was stronger than its ability to increasing the solute vapor pressure. In addition, a retrograde phenomenon reflecting the effect of temperature on solubility has been observed due to the decrease in density with the temperature of SC-CO₂ at constant pressure with temperature. However, the magnitude of such a density drop decreases at elevated pressures (Table 2). This retrograde solubility behavior agrees with that observed for other compounds in SC-CO₂ (Taher et al., 2014; Tomita et al., 2014).

3.5. Fitting of solubility data with three density-based semi-empirical models

To analyze the fictitious solubility data for apigenin, three density-based semi-empirical models proposed by Chrastil (1982), Bartle, Clifford, Jafar, and Shiltone (1991) and Kumar and Johnston (1988) were used in this study. The previous literature contains many examples of investigations of these three models (Khamda et al., 2013; Taher et al., 2014) due to their outstanding simplicity in fitting the solute solubility in a SC-CO₂ system.

3.5.1. Chrastil model

The theoretical solubility data for apigenin in the SC-CO₂ system were first fitted using the density-based equation proposed by Chrastil (1982). The fitted results of the theoretical solubilities of apigenin with the Chrastil model are tabulated in Table 3. The plots of $\ln Y^*_{\text{Apigenin}}$ versus $\ln \rho$ for four temperatures (32, 39, 47 and 56 °C) are straight lines whose slopes are identical and equal to a_1 (S. 3A). The other parameters, a_0 and a_2 , are further obtained by performing a multiple linear regression on the experimental solubility data of apigenin. The consistency of the model with the measured data can be seen in Table 3,

Table 3

Obtained fitting constants for three density-based correlations, and approximate heat of vaporization, total heat of solution and heat of solvation for apigenin.

1 ^a	n^d	a_0	$10^3 a_1$	a_2	AARD (%) ^c	$\Delta H_{T,C}^f$ (kJ/mol)
	20	-16.18	2408.86	-2160.59	2.96	17.96
2 ^b	n^d	b_0	$10^3 b_1$	b_2	AARD (%) ^c	$\Delta H_{T,K-J}^g$ (kJ/mol)
	20	-2.01	3.31	-2399.26	3.52	19.95
3 ^c	n^d	c_0	$10^3 c_1$	c_2	AARD (%) ^c	ΔH_{vap}^h (kJ/mol)
	20	9.16	6.36	-3584.85	5.41	29.80
						ΔH_{solv}^i (kJ/mol)
						-10.84

where P is the pressure (MPa); P_{ref} is 0.1 MPa, ρ is the density of the SC-CO₂ (kg/m³), ρ_{ref} is a reference density (700 kg/m³), T is the temperature (K), and a_0 , a_1 , a_2 , b_0 , b_1 , b_2 , c_0 , c_1 and c_2 are parameters.

^a Chrastil model: $\ln(y^*) = a_0 + a_1 \ln(\rho) + \frac{a_2}{T}$

^b K-J model: $\ln(y^*) = b_0 + b_1 \rho + \frac{b_2}{T}$

^c Bartle model: $\ln\left(\frac{y^* P}{P_{\text{ref}}}\right) = c_0 + c_1 (\rho - \rho_{\text{ref}}) + \frac{c_2}{T}$

^d Number of data points used in the correlation.

^e Average absolute relative deviation, $AARD(\%) = \frac{100}{n} \sum_{i=1}^n \left| \frac{y_{p,i} - y_{e,i}}{y_{e,i}} \right|$

^f Total heat of solution obtained from the Chrastil model.

^g Total heat of solution obtained from the K-J model.

^h Heat of vaporization obtained from the Bartle model.

ⁱ Heat of solvation, $\Delta H_{\text{solv}} = \frac{1}{2}(\Delta H_{T,C} + \Delta H_{T,K-J}) - \Delta H_{\text{vap}}$

and the value of overall AARD(%) is less than 2.96%. The results exhibited good agreement between the tested data and the calculations of the Chrastil model.

3.5.2. Kumar and Johnston model

According to the K-J model, all the theoretical solubilities at different temperatures will lie on a single straight line. The result shows that the self-consistency of the experimental data is satisfactorily determined using the K-J model (S. 3B). The results of fitting the theoretical solubilities of apigenin with the K-J model are tabulated in Table 3. As shown in Table 3, the model performs very well for the target compound in the SC-CO₂ system, with an overall AARD(%) of 3.52%.

Furthermore, the total heats of solution were estimated by the Chrastil equation or K-J equation and are given in Table 3. As shown in Table 3, the total heat of solution obtained from the K-J model is 19.95 kJ/mol, which is in excellent agreement with that obtained from the Chrastil model. Similar results have been reported in previous studies (Yamini & Moradi, 2011; Khamda et al., 2013).

3.5.3. Bartle model

The theoretical solubility data of apigenin were also fitted using another density-based semi-empirical equation proposed by Bartle et al. (1991) with only two parameters that are related isothermally to the experimental data. The correlations obtained using the Bartle model for apigenin are plotted as $\ln(y_2 P / P_{\text{ref}})$ versus $(\rho - \rho_{\text{ref}})$ (S. 3C). The results of fitting the theoretical solubilities of apigenin with the Bartle model are further tabulated in Table 3, which shows that this density-based model performs well for apigenin in the SC-CO₂ system with an overall AARD(%) of 5.41%.

The Bartle model explicitly includes an energy term of c_2 . As in the fitting to the Chrastil model and the K-J model, the heat of vaporization of the solute in the Bartle model was therefore approximated using parameter c_2 (Table 3). Based on the values of the total heat of solution and the heat of vaporization, the heat of solvation for apigenin in the SC-CO₂ system (Table 3) can be calculated from the difference between the heat of vaporization and the average of the total heats obtained by

the Chrastil and K–J models. These values for the target compound are listed in Table 3, which shows that the heat of solvation was -10.84 kJ/mol for the target compound in the SC-CO₂ system. This phenomenon occurs because vaporization is endothermic (plus), whereas solvation is exothermic (minus), and the heat of vaporization is much higher than the total heat of solvation for the target compound. This result is in agreement with earlier studies for different compounds (Khamda et al., 2013; Jin, Wang, Zhang, & Liu, 2012).

3.6. Kinetic modeling and thermodynamic parameters of activation

This model proposes that the extraction occurs in two successive stages. In the first stage, the solute is extracted quickly because of the scrubbing and dissolution caused by driving force of the fresh solvent. In the next stage, the extraction process becomes much slower, accomplished by the external diffusion of the remaining solute from the interior of the plant tissue into the solution. Considering a second-order rate law, the rate of dissolution for the analyte contained in the solid to diffuse into the solution can be described by Eq. (3) (Yang & Wei, 2015b).

$$\frac{dC}{dt} = k(C_s - C)^2 \quad (3)$$

where dC/dt is the residual analyte for a unit of time, k is the second-order extraction rate constant (g/mg-min), C is the set of analyte concentrations in the liquid extract at a given extraction time t (mg/g), and C_s is the equilibrium concentration for the target compounds in the liquid extract (mg/g).

The second-order rate law approximation with the initial and boundary conditions ($t = 0$ to t and $C = 0$ to C) yields the following theoretical equations:

$$\int_0^C \frac{dC}{(C_s - C)^2} = \int_0^t k dt \quad (4)$$

$$C = \frac{C_s^2 kt}{1 + C_s kt} \quad (5)$$

A linearized equation was obtained by rearranging Eq. (5) (Wei & Yang, 2014):

$$\frac{t}{C} = \frac{1}{kC_s^2} + \frac{t}{C_s} = \frac{1}{h} + \frac{t}{C_s} \quad (6)$$

where h (mg/g-min) is the initial extraction rate. When t approaches 0,

$$h = kC_s^2 \quad (7)$$

Experimental kinetic data for the extraction of apigenin from *S. barbata* D. Don using USC-CO₂ procedure are presented in Fig. 2A–E. These data clearly show that a pressure of 30 MPa (Fig. 2B) is the best extraction pressure for obtaining apigenin from *S. barbata* D. Don using the USC-CO₂ procedure, based its yield and extraction efficiency. The kinetic data obtained from Fig. 2B also showed that the amount of apigenin, as expected, increases with temperature (32–56 °C). However, the yield of apigenin obtained from the USC-CO₂ extraction of apigenin from *S. barbata* D. Don at 64 °C was lower than that at 56 °C. Therefore, 64 °C was not selected for the experimental kinetic data curves. The experimental data in Fig. 2B (30 MPa, 32–56 °C) were fitted into the second-order model, and the kinetic parameters were obtained to investigate the effect of temperature on the extraction process. Calculated kinetic and fit quality parameters for the second-order model are shown in Table 4. The initial extraction rate, h , and the parameter C_s in the second-order model increased as the temperature increased (32–56 °C). However, the rate constant (k) decreased with increasing extraction temperature (Yang & Wei, 2015b; Vetal, Lade, & Rathod, 2013). These results revealed that the rapid extraction of apigenin from *S. barbata* D. Don using the USC-CO₂ procedure can proceed at a lower temperature and greatly reduce the need for aqueous ethanol solution. Due to the mass transfer of convection, the USC-CO₂ procedure decreases the

Table 4

(A) Parameters of second-order kinetic model and (B) thermodynamic quantities of activation for the USC-CO₂ extraction of apigenin from *S. barbata* D. Don at various temperatures^a.

(A)					
P (MPa)	T ^b (°C)	h ^c (mg/g-min)	k ^d (g/mg-min) × 10 ⁻³	C _s ^e (mg/g)	R ^{2f}
30.0	32	0.048	8.091	2.443	0.93
	39	0.054	6.632	2.867	0.94
	47	0.055	6.363	2.948	0.93
	56	0.061	5.512	3.322	0.93
(B)					
P (MPa)	T (°C)	ΔH _a ^g (kJ/mol)	ΔS _a ^h (J/mol-K)	ΔG _a ⁱ (kJ/mol)	
30.0	32	-15.02	-334.63	87.09	
	39			89.43	
	47			92.11	
	56			95.12	

^a USC-CO₂ extraction conditions are fixed at a mean particle size of 0.355 mm, a pressure of 30.0 MPa with a CO₂ flow rate of 0.49 g/min and 12.6% of 80% ethanol in water (v/v) as a cosolvent for a 125-min extraction.

^b Extraction temperature.

^c Initial extraction rate.

^d Rate constant.

^e Equilibrium concentration.

^f $R^2 = \frac{\sum_{i=1}^n (y_{p,i} - y_{e,i})^2}{\sum_{i=1}^n (y_{p,i} - y_m)^2}$.

^g The enthalpy of activation.

^h The entropy of activation.

ⁱ The Gibbs free energy of activation.

energy barrier in the extraction process and enormously accelerates the extraction rate of apigenin.

The kinetics described in the previous equations depended on the extraction temperature and may be described using the Arrhenius equation (Wei & Yang, 2015):

$$k = Ae^{-Ea/R_g T} \quad (8)$$

where A is a temperature-independent factor (g/mg-min), Ea is the activation energy of extraction (kJ/mol), R_g is the gas constant (kJ/mol-K), and T is the absolute temperature (K). Consequently, the activation energy can be calculated from the slope of the straight line when plotting the logarithm of k against the reciprocal of absolute temperature (S.4). The activation energy for the USC-CO₂ extraction of apigenin from *S. barbata* D. Don was found to be -12.381 kJ/mol in the temperature range of 32–56 °C at a pressure of 30 MPa. This result indicates that the solute–solute cohesive and solute–solid adhesive interactions can be overcome to achieve solute transfer (Alupului, Călinescu, & Lavric, 2012).

According to the Eyring transition state theory (TST), the changes in the enthalpy of activation (ΔH), entropies of activation (ΔS), and Gibbs free energy (ΔG) of activation can be calculated using the following equations (Swati et al., 2013).

$$\Delta H_a = E_a - RT \quad (9)$$

$$\ln \frac{k}{T} = -\frac{\Delta H_a}{R} \times \frac{1}{T} + (\ln \frac{k_B}{h} + \frac{\Delta S_a}{R}) \quad (10)$$

$$\Delta G_a = \Delta H_a - T\Delta S_a \quad (11)$$

where ΔH_a is the enthalpy of activation (kJ/mol), E_a is the activation energy, ΔS_a is the entropy of activation (kJ/mol-K), ΔG_a is the Gibbs free energy of activation (kJ/mol), k_B is the Boltzman constant (1.38×10^{-23} J/K), h is the Planck constant (6.6256×10^{-34} J/s). The plot (S. 5) of $\ln(k/T)$ versus $1/T$ or four temperatures are straight lines whose slopes are identical and equal to $-\Delta H_a/R$. Furthermore, these thermodynamic parameters of activation for the USC-CO₂ extraction of apigenin from *S. barbata* D. Don are tabulated in Table 4.

4. Conclusion

This study investigated the combined procedure of ultrasound-assisted SC-CO₂ (USC-CO₂) extraction to improve the extraction efficiency of classic extraction techniques, such as heat-reflux and SC-CO₂ extraction, to extract apigenin from *S. barbata* D. Don. The results indicated that USC-CO₂ extraction was superior to the other extraction techniques, based on its higher extraction yield and extraction efficiency. The theoretical solubility of apigenin in the SC-CO₂ system, was also determined from the USC-CO₂ dynamic extraction and the retrograde solubility behavior occurs in the supercritical state for the compound of interest. Furthermore, the theoretical solubility data of apigenin were fitted well with three density-based models, Bartle, Chrastil and Kumar and Johnston models, with overall AARDs(%) of 5.41%, 2.96% and 3.52%, respectively. Based on the fitting results of the three density-based models, these three thermodynamic properties of the solid solute in the SC-CO₂ system can be conveniently estimated. In addition, the second-order model was used to interpret the kinetics data obtained from the USC-CO₂ procedure.

Acknowledgments

The authors thank the National Science Council of Taiwan (106-2914-I-041-001-A1 and 105-2914-I-037-012-A1), Kaohsiung Medical University (ORD, CRRD, etc.), Chuang Song Zong Pharmaceutical Co., Ltd (Kaohsiung, Taiwan) (KMU-M106034, KMU-M104020, S102035 and S102036) and Chia Nan University of Pharmacy and Science (Tainan, Taiwan) (151200-CN10527) for the financial support. We greatly thank Kaiser Pharmaceutical Co., Ltd (KPC, Tainan, Taiwan) for kindly providing and authenticating the plant materials used in this research. We thank our KMU colleagues (Li-Mei An, Shui-Chin Lu, Yen-Jung Lee, Min-Yuan Hung, Tin-Hsin Hsiao, Wen-Jeng Su, etc.) and students (Yi-Jing Jang, Chin-Wei Kuo, Chia-Chi Wu, Yu-Hung Chou, Chuan-Yu Wang, Yu-Hua Chang, etc.) for technical and editorial assistance. Finally, we acknowledge the editors and referees for their constructive comments and encouragement.

Conflict of interest

The authors declare no competing financial interest.

Appendix A. Supplementary data

Supplementary data associated with this article can be found, in the online version, at <http://dx.doi.org/10.1016/j.foodchem.2017.12.086>.

References

- Abrahamsson, V., Rodriguez-Meizoso, I., & Turner, C. (2015). Supercritical fluid extraction of lipids from linseed with on-line evaporative light scattering detection. *Analytica Chimica Acta*, *853*, 320–327.
- Albuquerque, B. R., Prieto, M. A., Barreiro, M. F., Rodrigues, A., Curran, T. P., Barros, L., & Ferreira, I. C. F. R. (2017). Catechin-based extract optimization obtained from *Arbutus unedo* L. fruits using maceration/microwave/ultrasound extraction techniques. *Industrial Crops and Products*, *95*, 404–415.
- Alupului, A., Călinescu, I., & Lavric, V. (2012). Microwave extraction of active principles from medicinal plants. *UPB Scientific Bulletin Series B*, *74*, 129–142.
- Bartle, K. D., Clifford, A. A., Jafar, S. A., & Shiltone, G. F. (1991). Solubilities of solids and liquids of low volatility in supercritical carbon dioxide. *Journal of Physical and Chemical Reference Data*, *20*, 713–756.
- Bosso, A., Guaita, M., & Petrozziello, M. (2016). Influence of solvents on the composition of condensed tannins in grape pomace seed extracts. *Food Chemistry*, *207*, 162–169.
- Chrastil, J. (1982). Solubility of solids and liquids in supercritical gases. *Journal of Physical Chemistry*, *86*, 3016–3302.
- Gao, Y., Nagy, B., Liu, X., Simándi, B., & Wang, Q. (2009). Supercritical CO₂ extraction of lutein esters from marigold (*Tagetes erecta* L.) enhanced by ultrasound. *Journal of Supercritical Fluids*, *49*, 345–350.
- Glisic, S. B., Ristic, M., & Skala, D. U. (2011). The combined extraction of sage (*Salvia officinalis* L.): ultrasound followed by supercritical CO₂ extraction. *Ultrasonics Sonochemistry*, *18*, 318–326.
- Hu, A. J., Zhao, S. N., Liang, H. H., Qiu, T. Q., & Chen, G. H. (2007). Ultrasound assisted supercritical fluid extraction of oil and coixenolide from adlay seed. *Ultrasonics Sonochemistry*, *14*, 219–224.
- Jin, J. S., Wang, Y. B., Zhang, Z. T., & Liu, H. T. (2012). Solubilities of benzene sulfonamide in supercritical CO₂ in the absence and presence of cosolvent. *Thermochimica Acta*, *527*, 165–171.
- Khamda, M., Hosseini, M. H., & Rezaee, M. (2013). Measurement and correlation solubility of cefixime trihydrate and oxymetholone in supercritical carbon dioxide (CO₂). *Journal of Supercritical Fluids*, *73*, 130–137.
- Klejduš, B., Lojková, L., Plaza, M., Šnoblóvá, M., & Štěrbóvá, D. (2010). Hyphenated technique for the extraction and determination of isoflavones in algae: ultrasound-assisted supercritical fluid extraction followed by fast chromatography with tandem mass spectrometry. *Journal Chromatography A*, *1217*, 7956–7965.
- Kumar, S. K., & Johnston, K. P. (1988). Modeling the solubility of solids in supercritical fluids with density as the independent variable. *Journal of Supercritical Fluids*, *1*, 15–22.
- Liau, B. C., Ponnusamy, V. K., Lee, M. R., Jong, T. T., & Chen, J. H. (2017). Development of pressurized hot water extraction for five flavonoid glycosides from defatted *Camellia oleifera* seeds (byproducts). *Industrial Crops and Products*, *95*, 296–304.
- Macías-Sánchez, M. D., Mantell, C., Rodríguez, M., Martínez de la Ossa, E., Lubian, L. M., & Montero, O. (2009). Comparison of supercritical fluid and ultrasound-assisted extraction of carotenoids and chlorophyll a from *Dunaliella salina*. *Talanta*, *77*, 948–952.
- Marcello, S. L., Monica, D. C., Pier, P. M., Andrea, L., Leonardo, R., Volker, B., ... Gabriella, P. (2015). Enzyme-aided extraction of lycopene from high-pigment tomato cultivars by supercritical carbon dioxide. *Food Chemistry*, *170*, 193–202.
- Martinez-Correa, H. A., Bitencourt, R. G., Kayano, A. C. A. V., Magalhães, P. M., Costa, F. T. M., & Cabral, F. A. (2017). Integrated extraction process to obtain bioactive extracts of *Artemisia annua* L. leaves using supercritical CO₂, ethanol and water. *Industrial Crops and Products*, *95*, 535–542.
- Moorthy, I. G., Maran, J. P., Ilakya, S., Anitha, S. L., Sabarima, S. P., & Priya, B. (2017). Ultrasound assisted extraction of pectin from waste *Artocarpus heterophyllum* fruit peel. *Ultrasonics Sonochemistry*, *34*, 525–530.
- Santos, P., Aguiar, A. C., Barbero, G. F., Rezendee, C. A., & Martínez, J. (2015). Supercritical carbon dioxide extraction of capsaicinoids from malagueta pepper (*Capsicum frutescens* L.) assisted by ultrasound. *Ultrasonics Sonochemistry*, *22*, 78–88.
- Swati, G., Haldar, S., Ganguly, A., & Chatterjee, P. K. (2013). Investigations on the kinetics and thermodynamics of dilute acid hydrolysis of *Parthenium hysterophorus* L. substrate. *Chemical Engineering Journal*, *229*, 111–117.
- Taher, H., Al-Zuhair, S., Al-Marzouqi, A. H., Haik, Y., Farid, M., & Tariq, S. (2014). Supercritical carbon dioxide extraction of microalgae lipid: Process optimization and laboratory scale-up. *Journal of Supercritical Fluids*, *86*, 57–66.
- Tao, G., & Balunas, M. J. (2016). Current therapeutic role and medicinal potential of *Scutellaria barbata* in Traditional Chinese Medicine and Western research. *Journal of Ethnopharmacology*, *182*, 170–180.
- Tomita, K., Machmudah, S., Wahyudiono, Fukuzato, R., Kanda, H., Qutain, A. T., Sasaki, M., & Goto, M. (2014). Extraction of rice bran oil by supercritical carbon dioxide and solubility consideration. *Separation and Purification Technology*, *125*, 319–325.
- Vetal, M. D., Lade, V. G., & Rathod, V. K. (2013). Extraction of ursolic acid from *Ocimum sanctum* by ultrasound: process intensification and kinetic studies. *Chemical and Engineering Processing*, *69*, 24–30.
- Wei, M. C., Yang, Y. C., Chiu, H. F., & Hong, S. J. (2013). Development of a hyphenated procedure of heat-reflux and ultrasound-assisted extraction followed by RP-HPLC separation for the determination of three flavonoids content in *Scutellaria barbata* D. Don. *Journal of Chromatography B, Analytical Technologies in the Biomedical and Life Sciences*, *940*, 126–134.
- Wei, M. C., & Yang, Y. C. (2014). Extraction characteristics and kinetic studies of oleonic and ursolic acids from *Hedyotis diffusa* using ultrasound-assisted extraction conditions. *Separation and Purification Technology*, *130*, 182–192.
- Wei, M. C., & Yang, Y. C. (2015). Kinetic studies for ultrasound-assisted supercritical carbon dioxide extraction of triterpenic acids from healthy tea ingredient *Hedyotis diffusa* and *Hedyotis corymbosa*. *Separation and Purification Technology*, *142*, 316–325.
- Wei, M. C., Lin, P. H., Hong, S. J., Chen, J. M., & Yang, Y. C. (2016). Development of a green alternative procedure for simultaneous separation and quantification of clove oil and its major bioactive constituents. *ACS Sustainable Chemistry & Engineering*, *4*, 6491–6499.
- Wei, M. C., Xiao, J., & Yang, Y. C. (2016). Extraction of α-humulene-enriched oil from clove using ultrasound-assisted supercritical carbon dioxide extraction and studies of its fictitious solubility. *Food Chemistry*, *210*, 172–181.
- Wei, M. C., Hong, S. J., & Yang, Y. C. (2017). Isolation of triterpenic acid-rich extracts from *Hedyotis corymbosa* using ultrasound-assisted supercritical carbon dioxide extraction and determination of their fictitious solubilities. *Journal of Industrial and Engineering Chemistry*, *48*, 202–211.
- Xie, X., Zhu, D., Zhang, W., Huai, W., Wang, K., Huang, X., ... Fan, H. (2017). Microwave-assisted aqueous two-phase extraction coupled with high performance liquid chromatography for simultaneous extraction and determination of four flavonoids in *Crotalaria sessiliflora* L. *Industrial Crops and Products*, *95*, 632–642.
- Yamini, Y., & Moradi, M. (2011). Measurement and correlation of antifungal drugs solubility in pure supercritical CO₂ using semiempirical models. *Journal of Chemical Thermodynamics*, *43*, 1091–1096.
- Yang, Y. C., Wei, M. C., & Huang, T. C. (2012). Optimisation of an ultrasound-assisted extraction followed by RP-HPLC separation for the simultaneous determination of oleonic acid, ursolic acid and oridonin content in *Rabdosia rubescens*. *Phytochemical Analysis*, *23*, 627–636.
- Yang, Y. C., Wei, M. C., Hong, S. J., Huang, T. C., & Lee, S. Z. (2013). Development/optimization of a green procedure with ultrasound-assisted improved supercritical carbon dioxide to produce extracts enriched in oleonic acid and ursolic acid from *Scutellaria barbata* D. Don. *Industrial Crops and Products*, *49*, 542–553.

- Yang, Y. C., Wei, M. C., Huang, T. C., & Lee, S. Z. (2013). Extraction of protocatechuic acid from *Scutellaria barbata* D. Don using supercritical carbon dioxide. *Journal of Supercritical Fluids*, *81*, 55–66.
- Yang, Y. C., Wei, M. C., Huang, T. C., Lee, S. Z., & Lin, S. S. (2013). Comparison of modified ultrasound-assisted and traditional extraction methods for the extraction of baicalin and baicalein from *Radix Scutellariae*. *Industrial Crops and Products*, *45*, 182–190.
- Yang, Y. C., Wei, M. C., & Hong, S. J. (2014). Ultrasound-assisted extraction and quantitation of oils from *Syzygium aromaticum* flower bud (clove) with supercritical carbon dioxide. *Journal Chromatography A*, *1323*, 18–27.
- Yang, Y. C., & Wei, M. C. (2015a). Ethanol solution-modified supercritical carbon dioxide extraction of triterpenic acids from *Hedyotis corymbosa* with ultrasound assistance and determination of their solubilities. *Separation and Purification Technology*, *150*, 204–214.
- Yang, Y. C., & Wei, M. C. (2015b). Kinetic and characterization studies for three bioactive compounds extracted from *Rabdosia rubescens* using ultrasound. *Food and Bioprocess Processing*, *94*, 101–113.
- Yang, Y. C., & Wei, M. C. (2016). A combined procedure of ultrasound-assisted and supercritical carbon dioxide for extraction and quantitation oleanolic and ursolic acids from *Hedyotis corymbosa*. *Industrial Crops and Products*, *79*, 7–17.
- Yang, Y. C., Lin, P. H., & Wei, M. C. (2017). Production of oridonin-rich extracts from *Rabdosia rubescens* using hyphenated ultrasound-assisted supercritical carbon dioxide extraction. *Journal of the Science of Food and Agriculture*, *97*, 3323–3332.
- Zhao, J., Deng, J. W., Chen, Y. W., & Li, S. P. (2013). Advanced phytochemical analysis of herbal tea in China. *Journal Chromatography A*, *1313*, 2–23.